

A SIMPLE BALLISTIC MODEL FOR PYROCLASTIC ERUPTIONS: APPLICATION TO THE MOON, MARS, AND IO. L. Keszthelyi¹, L. Gaddis¹, M. Hunter¹, L.M. Glaspie². ¹USGS Astrogeology Science Center, Flagstaff, AZ 86001. ²Dept. of Physics and Astronomy, Northern Arizona University, Flagstaff, AZ.

Introduction: This study is part of an ongoing investigation of small lunar pyroclastic deposits, including those in Alphonsus crater [1-3]. The modeling reported on here is being used to constrain the nature and quantity of the volatiles driving the eruptions. To test the model we also compare our results to some classic pyroclastic deposits across the Solar System.

Previous Ballistic Modeling: Modeling of pyroclastic eruptions is a well-established field. There are a number of sophisticated models for the ballistic flight of pyroclasts taking into account the effect of air drag and collisions between particles [e.g., 4,5]. However, when dealing with sporadic vulcanian or strombolian explosions in the airless environment of the Moon (and Io), a very simple analytical model is sufficient to provide useful insight. The model we employ is only a modest improvement over those used during the Apollo era [e.g., 6,7], the mathematics of which has been recently summarized by Glaze and Baloga [8].

A simple ballistic model predicts that the deposit is bimodal with thick deposits both at the vent and near the maximum extent of the deposit. The accumulation of material at the vent is primarily from particles that are ejected at near-horizontal angles with only a small component from particles that fly vertically and land back on the vent. Particles ejected in a near-horizontal direction have very short flight times and thus little time to cool. The rapid accumulation rate combined with the limited cooling of these near-vent deposits favors the formation of lava flows and ponds rather than pyroclastic constructs.

For the model to form more realistic pyroclastic deposits, it is necessary to exclude the near-horizontal trajectories. As [8] summarizes, there are three styles of deposits that form as the ejection angle is progressively restricted. If the angles are tightly restricted, a relatively uniform deposit is formed. As the angle widens toward 45°, the thickening at the outer edge of the deposit becomes very pronounced. As the angle continues to widen, a broader inner annulus forms, producing a 3-ringed bull's-eye pattern of successively thicker deposits. This pattern is expected to be diffused by variations in the initial speed (V_o) of the particles.

Additions to the Model: Our model makes one minor change from previous models in that it explicitly uses topography as the means of restricting the ejection angles. As the source of the explosions moves deeper beneath the surface, the more horizontal trajectories are truncated, creating the patterns of deposits described by [8]. This change allows us to analytically examine the

effect of local topography on the outline of ballistic deposits, following up on earlier numerical modeling [9].

Application to Alphonsus Crater: Table 1 uses some of the new estimates of the extent of the pyroclastic deposits from [2]. Using the common assumption that the pyroclasts' V_o equals the final speed of the gas expanding into a vacuum, ~0.4 wt.% CO or CO₂ is required. Only ~1/2 as much H₂O or 1/10th as much H₂ is needed because of those gasses' lower molecular weights. For a mix of volcanic gasses including sulfur and halogens, the mass fraction is ~0.1-0.3 wt.%. These amounts are very reasonable for lunar basalts [e.g., 10], so it is not necessary to call upon special processes to accumulate gas for these eruptions. This does depend on the assumption that V_o equals the final gas speed.

Table 1. Size and initial speed of Alphonsus pyroclastic deposits. See [2] for more details on morphometry.

Crater	Depth (m)	Deposit Radius (m)	V_o (m/s)
Ravi	210	3640	78.8
Alphonsus	260	5840	99.2
Soraya	350	4340	87.0

At Soraya, the dark deposit is truncated to the NE against a >300 m tall escarpment at a distance of ~2500 m compared to the average distance of 4340 m (Fig. 1). The model predicts that the ballistic paths should have been shortened by ~500 m instead of the observed 1000 m (Fig. 2). This suggests that topography restricted the deposit but the current extent is further reduced by subsequent mass wasting that buried any pyroclastic material that was deposited on the escarpment's slopes.

Figure 1. Brightness and topographic profiles across the Soraya deposit where it interacts with a local scarp. See [2] for details of the data and methods.

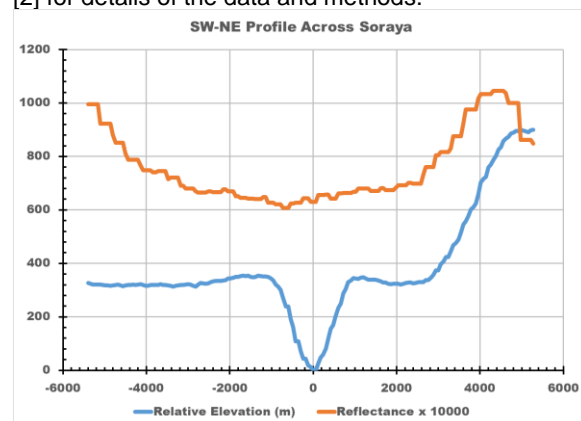
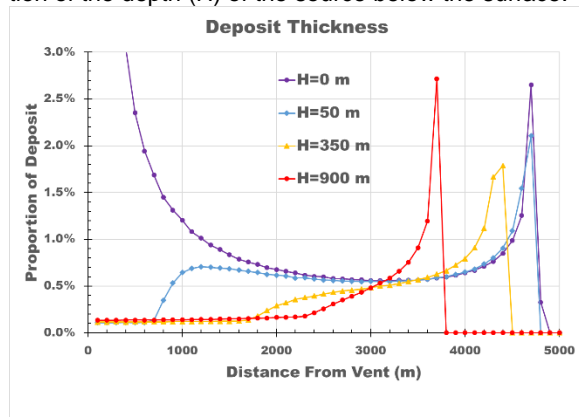


Figure 2. Ballistic deposit thickness profiles as a function of the depth (H) of the source below the surface.



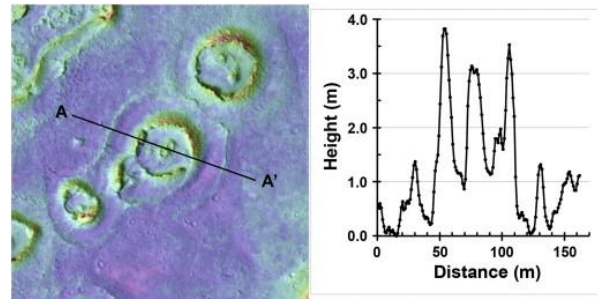
It is noteworthy that none of the reflectance or spectral profiles of the dark diffuse deposits in this region show evidence of thickening outward in a step-wise fashion. Instead there is a smooth outward brightening and reduction in the spectral signature of volcanic glass [3]. This is not what is expected from a simple eruption consisting of a short series of similar strombolian or vulcanian explosions. A vulcanian eruption with explosions that successively excavated a crater might be able to produce the observed deposit profile. An alternative is a longer-lived, perhaps Hawaiian-style, eruption with a brief waxing and long gradual waning period. It is also possible that the diffuse outer margin of the deposits is the result of impact gardening and lateral transport.

Application to Orientale Ring: This ~30 km wide, dark ring with a maximum radius of ~80 km has previously been shown to be consistent with a ballistically emplaced pyroclastic deposit with the minimum ejection angle close to 45° [9, 11]. To get material out to ~80 km, V_o must have been ~360 m/s. However, to put the inner edge of the ring at ~50 km, the analytical model suggests a ~15 km depth for the eruptive source and V_o needs to be raised to ~400 m/s. The gas fraction ranges from ~10 wt.% for a sulfur/halogen-rich gas to ~0.5 wt.% for H_2 . While this crude model gives a three times greater depth than [11], the results are surprisingly similar: the deposit requires an eruption where gas-enriched magma degassed explosively in a deep-throated vent.

Application to Pele: This 1200 km-diameter red ring of short-chained sulfur is one of the most prominent features on Io. The deposit is remarkably stable and long-lived, characteristics consistent with the bubbling lava lake source that was imaged by Galileo [12]. The ballistic model suggests a V_o of ~1000 m/s and ~50 wt.% gas. This fits the hypothesis that the sulfur particles are condensing from expanding sulfur-rich gas and are not primary pyroclasts [13].

Application to Athabasca Valles Rootless Cones: HiRISE images have revealed numerous phreatovolcanic constructs throughout Athabasca Valles [14]. It has been previously noted that the features are smaller at higher elevation and larger on the floor of the valley, consistent with steam pressure being proportional to the lava overburden. The multi-ringed nature of many of the constructs (Fig. 3) has not had a simple explanation. The model suggests that these well-developed rings are the product of a series of very uniform bubble bursts. The inner and outer rings could have formed together if the depth of the explosions was very shallow, creating a bimodal deposit. The model predicts V_o 's of 5-15 m/s impelled by ~0.01 wt.% gas. The low modeled gas fraction could reflect poor coupling between the gas and the relatively briefly accelerated large spatter particles.

Figure 3. HiRISE DTM and topographic profile of a rootless cone on the floor of Athabasca Valles.



Conclusion: Despite its limitations, this very simple model is surprisingly capable of providing order of magnitude estimates for explosive eruptive processes across the Solar System. Based on these model results, we suggest that, unlike the Orientale ring, the Alphonso crater pyroclastic deposits could be the result of common eruptive processes for lunar basalts. Similar near-vent pyroclastic deposits may have been a far more common part of the Moon's volcanic history than previously recognized.

References: [1] Gaddis L. R. et al. (2016) LPS XLVII, Abstract #2065. [2] Hunter M. A. et al. (2018) LPS XLIX, this meeting. [3] Glaspie L. M. et al. (2018) LPS XLIX, this meeting. [4] Broz P. et al. (2014) *EPSL*, 406, 14-23. [5] Tsunematsu, K et al. (2013) *Comp. Geosci.*, 63, 62-69. [6] Head J. W. (1975) *LPS VI*, 349. [7] Head J. W. and Wilson L. (1979) *Proc. LPS Conf. 10th*, 2861-2897. [8] Glaze L. S. and Baloga S. M. (2000) *JGR*, 105, 17,579-17,588. [9] Gaddis L. et al. (2013) LPS XLIV, Abstract #2587. [10] McCubbin, F. M. et al. (2015) *American Mineral.*, 100, 1668-1707. [11] Head J. W. et al. (2002) *JGR* 107, 10.1029/2000JE001438. [12] Radebaugh J. et al. (2004) *Icarus*, 169, 65-79. [13] Spencer J. R. et al. (2000) *Science*, 288, 1208-1210. [14] Jaeger W. L. et al. (2007) *Science*, 317, 1709-1711.